



Thermal, structural and magnetic properties of $\text{TeO}_2\text{-MgO-Na}_2\text{O-Nd}_2\text{O}_3$ glass system with NiO nanoparticles



N.A.M. Jan^a, M.R. Sahar^{a,*}, Sulhadi Sulhadi^b, R. El-Mallawany^c

^a Advanced Optical Material Research Group, Department of Physics, Faculty of Science, Universiti Teknologi Malaysia, 81310 Skudai, Johor, Malaysia

^b Physics Department, Universitas Negeri Semarang, Semarang 50229, Indonesia

^c Physics Department, Faculty of Science, Menoufia University, Egypt

ARTICLE INFO

Keywords:
Tellurite glass
Nickel oxide nanoparticles
Thermal
Structural
Hysteresis loop

ABSTRACT

In this work, we have five samples of NiO Nanoparticles (NPs) embedded in tellurite glass system of composition Neodymium doped tellurite nanostructured glass having a composition of $(72.5-x)\text{TeO}_2\text{-}15\text{MgO}\text{-}10\text{Na}_2\text{O}\text{-}2.5\text{Nd}_2\text{O}_3\text{-}(x)\text{NiO}$, $x = 0.5, 1.0, 1.5, 2.0, 2.5$ mol% has successfully been completed by melt-quenching procedure. Structure of crystallization is determined using XRD technique verifies amorphous natures of produced glass. Differential thermal stability analyser (DTA-Parkin-Elmer) is utilized to illustrate the thermal stability of a sample at a temperature ranged from 300 to 600 °C. A Transmission Electron Microscope (TEM) is used to detect the presence of NiO NPs and High-Resolution Transmission Microscope (HRTEM) is utilizing to measure the d-spacing of the NPs. The structure in glass network is identified by FT-IR and Raman spectrometer. The elemental trace in the glass sample is detected using the energy dispersive of X-ray (EDX) analysis. Meanwhile, magnetization measurements are carried out using Variable sample magnetometer (VSM). The transition temperature, T_g is found at 388 °C, the melting temperature T_m is ranged at 530–540 °C depending on composition while the thermal stability is around 117 °C. The structural and magnetic properties of the glass samples are observed to be delicate to NiO NPs concentration variations. The d-spacing at (111) plane having a size of 0.24 nm proves the presence of NiO NPs. The glass network contains of bending vibrations of Te-O-Te linkages centred at 448 cm^{-1} which is also the stretching band of NiO mode. It is also found that the glass structure is dominated with the existence of TeO_3 , TeO_{3+1} and TeO_4 tribypyramidal. The glass system reveals paramagnetic behaviour by magnetic hysteresis at room temperature with H_c values were observed to be decreased from 610 ± 30.5 to 139 ± 6.95 (Oe) and ratio of (Mr/Ms) from 0.153 ± 0.008 to 0.071 ± 0.004 with the increase of NiO NPs concentration.

1. Introduction

International progress in tellurite glasses modified with rare earth oxides (R.E.) or transition metal ion (T.M.) have been published caused by their interesting properties [1–5]. Tellurite glass is widely known due to better glass stability, high non-linear refractive index, highly corrosion resistance and unaffected to moisture for long periods compare to those of silicate, phosphate and fluoride glasses relatively. This implies that tellurite glasses are suitable for optical fibres, modulators, non-linear and laser applications [6–8]. Tellurium oxide is considered as alluring hosts for dynamic medium, considering their low phonon vitality and low liquefying temperature. So, adding a glass modifier enhances glass formation ability (GFA) through the breaking chain of structural unit and changes in structural formation unit. Neodymium doped phosphate laser glass had been used in many commercial

applications [9,10]. However, the phosphate host materials are known to be lack of durability, thus it need to be substituted with more suitable host materials. The combination of tellurite oxide and neodymium oxide offers novel and high optical efficiency in laser glass [11].

Recent technological applications have generated more attraction in the studies of NPs of magnetic materials due to their properties which usually vary from bulk materials. They have important applications in magnetic data-storage media, in magnetic liquids (ferrofluids), i.e. stable suspensions of magnetic NPs, in magnetic beads that are applied in biotechnology, for contrast enhancement in magnetic resonance imaging (MRI), and for the target drug delivery [12]. In this regard, tellurite glasses embedded with magnetic metallic NPs system has also gained a massive interest. The incorporation of magnetic metal NPs in glass improve the electrical field around rare earth and produce quantum effect to increase the optical efficiency of the glass system

* Corresponding author.

E-mail address: mrahim057@gmail.com (M.R. Sahar).

[13]. Among magnetic metal NPs, NiO NPs are particularly attractive due to their beneficial magnetic and electronic properties. They can be applied in the gas sensor, lithium - ion battery, p - type semiconductors (cubic, 3.5 eV), alkaline battery cathode and electrochemical capacitors [14–16]. It also exhibits anodic electrochromy, excellent durability, electrochemical stability, and high optical spin density. A recent study on NiO NPs has shown that NPs with an average diameter of 3–24 nm exhibit superparamagnetic along with magnetic hysteresis under a blocking temperature [17]. Other reported that small amount of NiO particles were known to be super - paramagnetic [18] while for pure NiO, it exhibits antiferromagnetic ordering with plane of opposite spin [19].

Although the behaviour of local environment of NiO NPs has been well established, advanced investigation on the influence of NiO NPs embedded in tellurite glass on the structural characteristics and magnetic properties are still deficient. Thus, in this research, the thermal, structural and magnetic properties of (72.5-x)TeO₂-15MgO-10Na₂O-2.5Nd₂O₃-(x)NiO glasses are studied using XRD, TEM, HRTEM, EDX, DTA, FTIR and Raman spectroscopy techniques. All the results will be discussed in detail with respect to composition.

2. Experimental work

The glasses with nominal composition of (72.5-x)TeO₂-15MgO-10Na₂O-2.5Nd₂O₃-xNiO with x = 0.5, 1.0, 1.5, 2.0, 2.5 mol% are made through melt quenching method. By mixing the oxides, batches of 20 g of well - mixed starting materials were prepared. Then, the well - mixed raw material is melted in an electric furnace at 900 °C in platinum crucible for half an hour. After that, the melts were quenched on a pre-heated stainless-steel mould at 300 °C before cooling gradually down to the room temperature. The obtained glass samples are named as 0.5NiO, 1.0NiO, 1.5NiO, 2.0NiO and 2.5NiO for x = 0.5, 1.0, 1.5, 2.0, and 2.5 respectively. The X-ray diffraction (XRD) measurement is done on a relatively fine powder by CuK α radiation at 40 kV, 30 mA utilizing Siemens Diffractrometer D5000 to identify the amorphous nature of glass. The differential thermal stability analyser (DTA-Parkin-Elmer) is utilized to illustrate thermal stabilities of sample in the range of 300–600 °C. The energy dispersive X-ray spectrometer (model Swift ED3000 EDX) was utilized to perceive elemental traces of glass samples. The existence of NiO NPs is noticed utilizing Transmission Electron Microscope (TEM) (model Philips CM12 along with Docu Version 3.2 and High-Resolution Transmitted Electron Microscope (HRTEM)functioned at a voltage acceleration of 20 kV. All infrared spectrum of the glass is noted at the room temperature (25 °C) utilizing a Perkin-Elmer Spectrum on FTIRspectrometer over the ranged 4000–400 cm⁻¹by 10 scans419at 4 cm⁻¹ resolutions. The Raman spectra are measured through a confocal Horiba Jobin Yvon (HR800 UV) at the spectral ranged 200–2000 cm⁻¹, with the laser power on the samples being 1000 mW. Magnetization measurements are carried out using Variable Sample Magnetometer (VSM).

3. Result and discussions

Table 1 shows the formation, colour and transparency of produced glass samples (72.5-x)TeO₂-15MgO-10Na₂O-2.5Nd₂O₃-(x)NiO, x = 0.5, 1.0, 1.5, 2.0, 2.5 mol%. All samples are transparent and slightly change in colour from green yellowish to light brown. **Fig. 1** displays the disordered nature of the glass sample in the 2.5NiO glass spectra as confirmed by XRD measurement. The XRD pattern verifies the glass is in the amorphous states, as indicated by the absence of sharp peaks with a broad hump for 2θ around the region 20–35°. **Fig. 2(a)** demonstrates the TEM images for 2.5NiO glass. The selected area in **Fig. 2(a)** is acceptable to predict the size of NiO NPs. Some black non-spherical spots having various shapes and sizes are visibly distributed inside the glass network. The inset of the **Fig. 2(a)** demonstrates the size of NiO NPs is observed to be gaussian having an average diameter 4.9 nm. **Fig. 2(b)**

clearly shows the sample SAED pattern suggesting strong bright diffraction spots revealed single crystalline cubic nickel oxide formation [20–23]. The appearance of NiO NPs lattice spacing for sample in HRTEM image is shown in **Fig. 2(c)**. The estimated distance between crystal lattice spacing is about 0.24 nm corresponding to (111) crystal facet of NiO NPs which matched with JCPDS card no. 00-004-0835 [24] and 03-065-5745. **Fig. 2(d)** demonstrates an optical absorption spectrum of the bulk samples (~2.0 mm thick) with seven absorption bands of; (²P_{1/2}, ²D_{5/2}), (⁴G_{7/2}), (⁴G_{5/2}, ²G_{7/2}), (⁴F_{9/2}), (⁴S_{3/2}, ⁴F_{7/2}), (²H_{9/2}, ⁴F_{5/2}) and (⁴F_{3/2}) as explained in previous report [25]. It can be seen in the present glasses that optical absorption edge has no sharp peaks indicates their glassy nature [26]. It is observed that the cut-off wavelength is in the range of (367–370) nm which indicate the limiting absorption at UV range. This result is in agreement with the other tellurite glass system reported elsewhere [27].

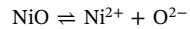
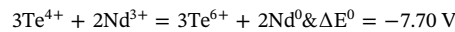
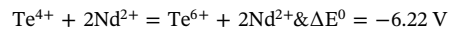
Creation of NiO NPs is ascribed to nucleation and growth and process, where potential for reducing redox system elements is demonstrated as follows:

$$\text{Nd}^{3+}/\text{Nd}^{2+} = 2.6 \text{ V}$$

$$\text{Nd}^{3+}/\text{Nd}^0 = -2.32 \text{ V}$$

$$\text{Te}^{6+}/\text{Te}^{4+} = 1.02 \text{ V}$$

The reduction procedures involved areas follows:



where ΔE^0 is the total of reduction process. Furthermore, NiO does not have ΔE^0 due to the bonding between Ni and O cannot be broken. The existence of NiO NPs in a glass may be strengthened by HRTEM lattice spacing, TEM images and EDX result. The calculated optical spectrum of nanosized nickel SPR absorption was reported to be between 300 and 400 nm [28]. Besides, this result is consistent with other reports [29,30]. **Fig. 3(a)** illustrates the distribution of elements in 2.5NiO glass. It can seemly be observed that Te, Mg, Nd, and Ni elements are randomly distributed among each other in scale of 5 μm image. However, the blue colour for these NPs cannot be seen clearly because of too small particle size (~ 4.9 nm) of NiO NPs and low composition content of NiO (2.5 mol%), in line with **Fig. 1** that cannot be detected by XRD either. However, EDX spectrum reveals some weak peaks of Ni from spectra as shown in **Fig. 3(b)**. **Table 2** encapsulates the details of the data collected from EDX. It shows the experimental and calculated weight of elements for the 2.5NiO glass sample. From **Table 2**, it can be seen that some Ni elements are detected which confirmed that the black spots showed in **Fig. 2(a)** are indeed NiO NPs.

Fig. 4 shows the DTA thermogram for the present (72.5-x)TeO₂-15MgO-10Na₂O-2.5Nd₂O₃-(x)NiO, x = 0.5, 1.0, 1.5, 2.0, 2.5 mol% and glass crystallization temperature (T_c), transition temperature (T_g) and melting temperature (T_m) have been tabulated in **Table 3**. It indicates one blunt endothermic hump pertaining to T_g at about 338 °C which due to arrangement of NiO in the glass system [31]. Another endothermic band is corresponded to T_m in the range 530–540 °C. The exothermic peak at about 455 °C is translated for T_c. The glass stability (ΔS) and the Hruby (H_R) are the ways to evaluate the glass thermal stability [32]. These equations are defined as follows [33]:

$$\Delta S = (T_c - T_g) \quad (1)$$

$$H_R = (T_c - T_g)/(T_m - T_c) \quad (2)$$

The ΔS of 2.5% NiO discovered the maximum thermal stability around 117 °C which is considered to be stable, in good agreement with the preceding value of ΔS when it is > 100 °C [34]. While the value of H_R is 1.52 that can be defined as the denominator of growth rate and nucleation rate [32]. These values are also consistent with the one

Table 1

The nominal composition of $(72.5-x)\text{TeO}_2\text{-}15\text{MgO}\text{-}10\text{Na}_2\text{O}\text{-}2.5\text{Nd}_2\text{O}_3\text{-}(x)\text{NiO}$, where $0 \leq x \leq 2.5$ mol% glasses.

Sample No.	Nominal composition (mol%)					Color	Samples figure
	TeO_2	MgO	Na_2O	Nd_2O_3	NiO		
TMNN1	72.0	15.0	10.0	2.5	0.5	Transparent, yellow	
TMNN2	71.5	15.0	10.0	2.5	1.0	Transparent, yellow	
TMNN3	71.0	15.0	10.0	2.5	1.5	Transparent, light brown	
TMNN4	70.5	15.0	10.0	2.5	2.0	Transparent, brown	
TMNN5	70.0	15.0	10.0	2.5	2.5	Transparent, brown	

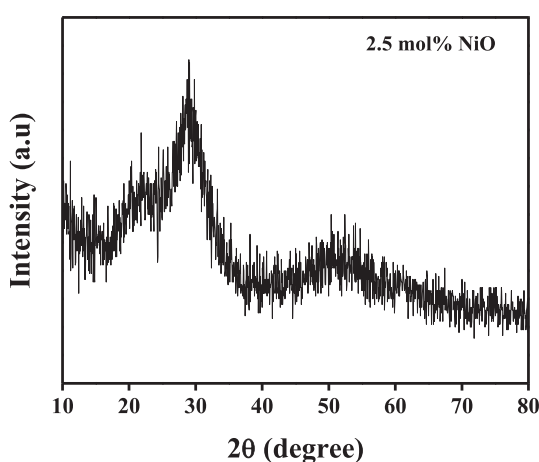


Fig. 1. XRD pattern of glass 2.5NiO.

reported by R. El-Mallawany [34].

Fig. 5 shows FTIR spectra of the present glass samples with 0.5, 1.0, 1.5, 2.0, 2.5 mol% of NiO NPs in a range of $400\text{-}2000\text{ cm}^{-1}$. Table 4 abridges the illustrated peak at the whole spectral area and correlating band assignment. Any band centred at around 448 cm^{-1} is allocated to combined bending vibration of the O-Te-O or Te-O-Telinkage [35]. This band also allocated to stretching NiO mode [36,37]. The broadening band in between 610 and 680 cm^{-1} is suggested due to Te-O stretching vibration of TeO_4 trigonal bipyramidal unit with connecting oxygen [38]. With a gradual increase in concentration of NiO, the TeO_4 band shifted to lower number corresponding to a reduction in the number TeO_3 units [39]. Meanwhile, the other band centred at 702 cm^{-1} matches to a transitional coordination of tellurium atom between 4 and 3 [40]. The shoulder band appearance at 766 cm^{-1} is attributed to TeO_3 trigonal pyramidal (tp) units with non-bridging oxygen inside glass network.

As a complementary technique to the infrared spectra, Raman spectrum of present glass system with 0.5, 1.0, 1.5, 2.0, 2.5 mol% of NiO NPs is shown in Fig. 6. (a) Raman patterns consisting of broad peaks in a range: 550 to 950 cm^{-1} and 300 to 550 cm^{-1} . Fig. 6. (b) shows the deconvolution of the Raman spectra of 2.5 mol% NiO NPs

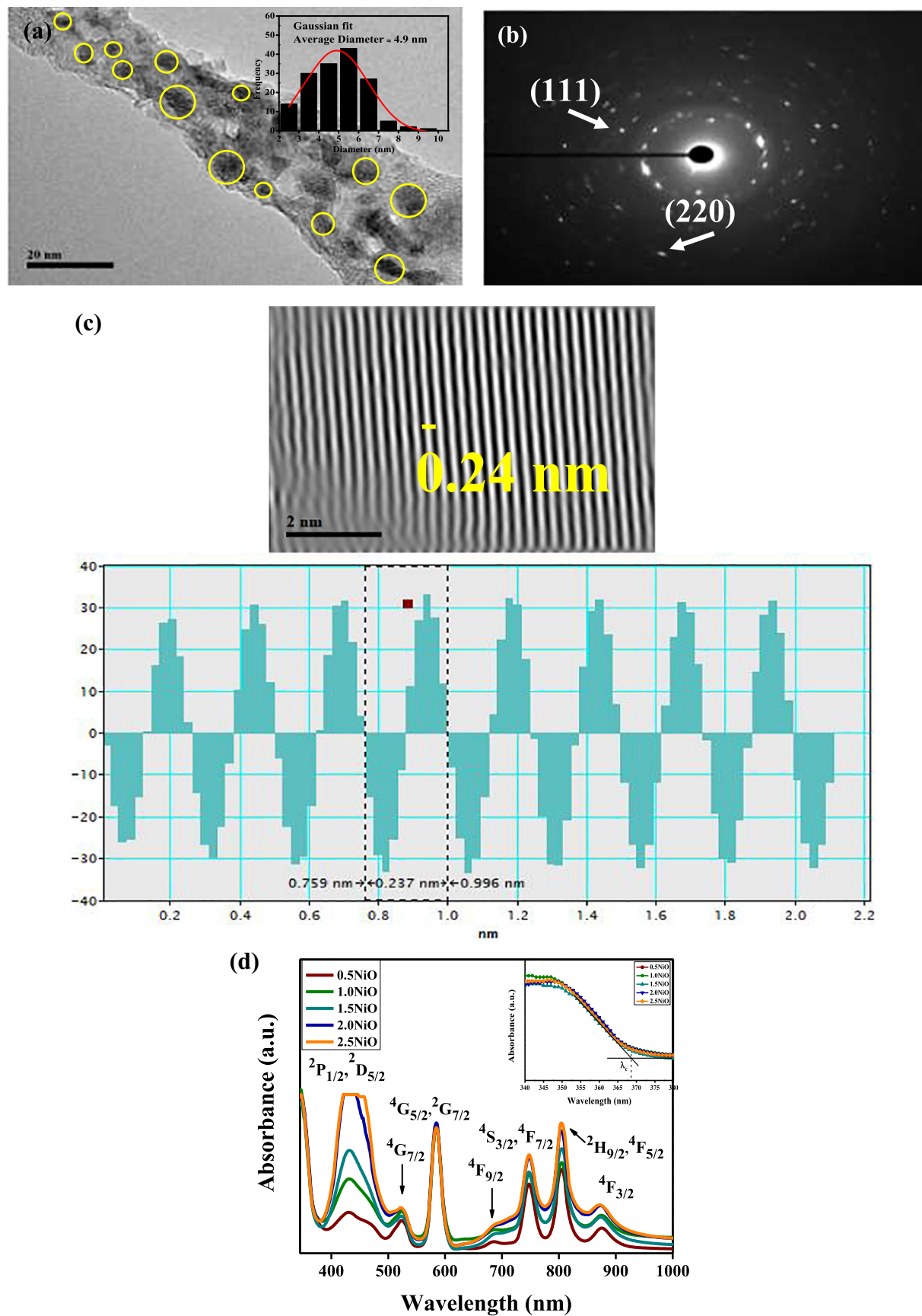


Fig. 2. (a) TEM images displaying the distribution of non-spherical NiO NPs (inset shows corresponding size distribution). (b) SAED pattern of 2.5NiO glass. (c) HRTEM image and the lattice fringe profile of 2.5NiO glass. (d) UV absorption spectra of glass samples (inset illustrating cut off wavelength of glass samples).

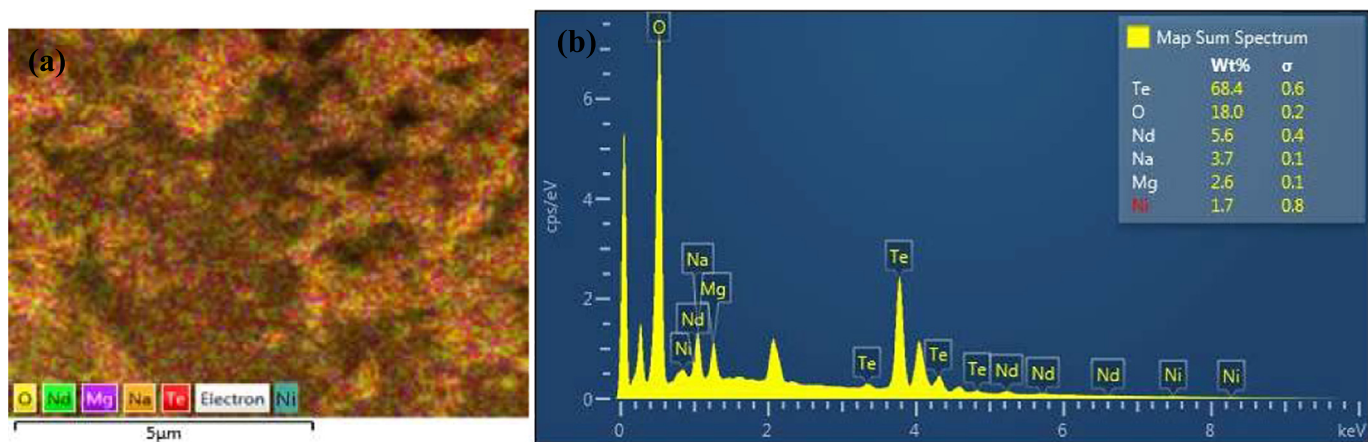


Fig. 3. (a) The distribution (b) EDX spectrum of elements Te, Mg, Na, Nd and Ni in 2.5NiO glass.

Table 2
Experimental and calculated weight of elements for the 2.5NiO glass sample.

Element	Experimental		Calculated	
	Wt%	Atomic%	Wt%	Atomic%
Na	3.69	8.03	4.50	18.43
Mg	2.55	5.26	3.11	12.07
Ni	1.74	1.49	2.12	3.42
Te	68.40	26.85	83.45	61.63
Nd	5.59	1.94	6.82	4.45

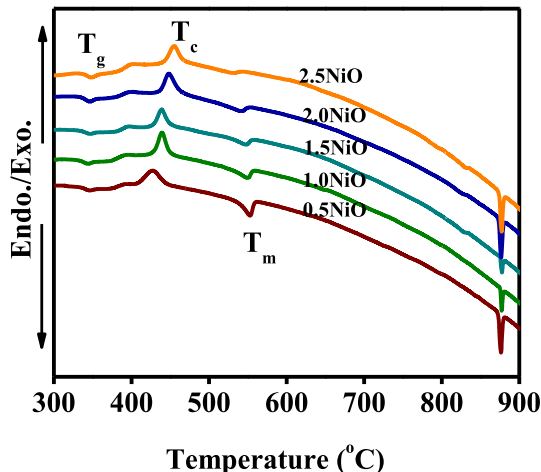


Fig. 4. DTA curve of glass samples.

Table 3
Glass transition temperature (T_g), crystallization temperature (T_c) and melting temperature (T_m) of $(72.5-x)\text{TeO}_2\text{-}15\text{MgO}\text{-}10\text{Na}_2\text{O}\text{-}2.5\text{Nd}_2\text{O}_3\text{-}(x)\text{NiO}$, where $0 \leq x \leq 2.5$ mol%.

Sample no	Temperature (± 0.01 °C)		
	T_g	T_c	T_m
TMNN1	334.46	427.56	552.72
TMNN2	330.83	439.47	549.44
TMNN3	333.47	438.63	547.68
TMNN4	334.06	448.19	541.79
TMNN5	337.86	454.91	531.78

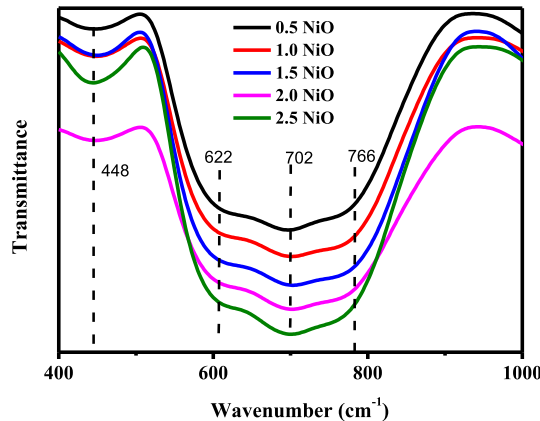


Fig. 5. NiO NPs content (mol%) dependent IR transmission bands of glass samples.

with baseline is corrected and peaks are centred at 464, 689, and 789 cm⁻¹. The assignment of Raman band is summarized in the Table 5. In the frequency range of 300 to 550 cm⁻¹, the existence of bending vibrations of Te-O-Te and O-Te-O linkage is observed at about 464 cm⁻¹ with O at a position alternatively equatorial and axial [41,42]. The strong band that appeared at peak around 689 cm⁻¹ is ascribed to stretching vibrational modes of TeO₄ tetrahedral with bridging oxygen (BO) atoms. It has been proposed that this band determined to a coupled symmetric vibration along Te-O-Te axis in the TeO₃₊₁/TeO₄ unit and TeO₄/TeO₃ pair [43]. Meanwhile, it has been considered that band to be related measure of connectivity among TeO₄, TeO₃ and TeO₃₊₁ species [44]. A Raman band centred at 789 cm⁻¹ can be assigned to the TeO₃ or TeO₃₊₁ units [42,45,46]. Increasing the NiO content of samples results in a shift to higher wave numbers from 752 cm⁻¹ when $x = 0.5$ mol% to 789 cm⁻¹ when $x = 2.5$ mol%. This is because an increase in the NiO content increases the quantity of non-bridging oxygen atom and transforms of TeO₄ to TeO₃ and TeO₃₊₁ structural unit in glass networks [44,47].

Fig. 7 displays the set of glass system hysteresis loop data obtained from magnetization M versus field H. It can be said that, the glass system at room temperature is an indication of paramagnetic behaviour. It is also in a similar trend with the hysteresis loop as reported previously [48]. The value of their remnant magnetization (Mr), saturation magnetization (Ms) and the coercivity field (Hc) can be found from the curve which are listed in Table 6. The obtained values of Ms. of bulk Ni (77.65 emu/g) [49] and Ni-Co oxide NPs [50] at room temperature are much higher than Ms. of glass system because of the implication of the non-magnetic surfactant coated [51]. It is might be due

Table 4

IR band assignments of $(72.5-x)\text{TeO}_2\text{-}15\text{MgO}\text{-}10\text{Na}_2\text{O}\text{-}2.5\text{Nd}_2\text{O}_3\text{-}(x)\text{NiO}$, where $0 \leq x \leq 2.5$ mol% glass samples with varying concentration of NiO NPs.

Glass					Band assignments
0.5NiO	1.0NiO	1.5NiO	2.0NiO	2.5NiO	
448	450	448	444	448	Bending vibrations of Te-O-Te
622	618	616	614	614	Stretching vibrations of Te-O of TeO_4
696–698	702	702–704	702	700–702	Stretching vibrations of Te-O of TeO_{3+1}
764	764	766	774	774	Stretching vibrations of Te-O of TeO_3 units

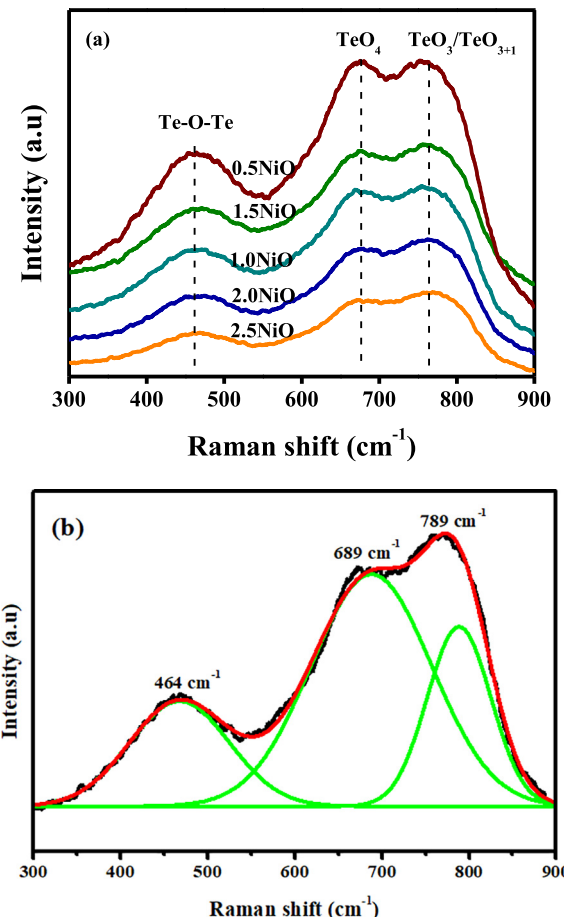


Fig. 6. (a) Raman spectra of $\text{TeO}_2\text{-MgO-Na}_2\text{O-Nd}_2\text{O}_3\text{-NiO}$, (b) the deconvolution of the Raman spectra of 2.5NiO.

Table 5

Assignments of Raman bands of glass samples $(72.5-x)\text{TeO}_2\text{-}15\text{MgO}\text{-}10\text{Na}_2\text{O}\text{-}2.5\text{Nd}_2\text{O}_3\text{-}(x)\text{NiO}$, where $0 \leq x \leq 2.5$ mol%.

Glass					Band assignments
0.5NiO	1.0NiO	1.5NiO	2.0NiO	2.5NiO	
457	471	469	469	464	Bending vibrations of Te-O-Te and O-Te-O
671	675	670	679	689	Stretching vibrations of TeO_4
752	752	757	764	789	Stretching vibrations of TeO_3 or TeO_{3+1}

to disorder canting spin (Spin-glass-like) onto the exterior of NiO NPs [52]. From Fig. 8(a), it was found that H_c value decreases as NiO NPs increase, which can be attributed to the effects of porosity that work as a demagnetizing field generator. A higher field is required to push that domain wall by decreasing the porosity and thus decreasing H_c [53]. According to Brown's relation [54] as per below,

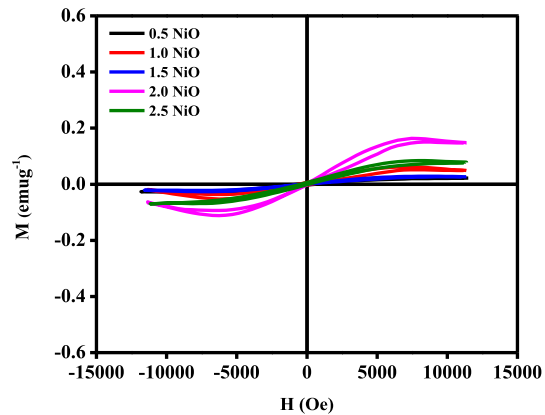


Fig. 7. The magnetic hysteresis loops (M - H curve) of NiO NPs embedded in tellurite glass.

H_c varying inversely to M_s , which in accordance with current result and similar for NiFe_2O_4 prepared by others [53].

$$H_c = 2K_1/\mu_0 M_s \quad (3)$$

Therefore, a rising trend of both M_s and M_r are shown in Table 6 with an increased concentration of NiO NPs. Which clearly shows that changes NPs local field environment and their electron spins can lead to an increase in M_s in the NiO NPs [55]. The comparison of the present values to other glass systems revealed higher values than phosphate glasses containing nickel NPs [49]. The modification of (M_r/M_s) as a function of NiO NPs concentration is presented in the Fig. 8(b). The (M_r/M_s) is an extent of how square a hysteresis loop is, which proposed a dominant role performed by an uniaxial magnetocrystalline anisotropy [56]. It is typically related with the bigger particles and the formation of domain - walls and high texture value [57]. The lower values of (M_r/M_s) in the range 0.01 to 0.1 indicates that the materials are in multidomain magnetic grains composed in the structure of the present tellurite glasses.

4. Conclusion

Transparent tellurite glass samples in the form $(72.5-x)\text{TeO}_2\text{-}15\text{MgO}\text{-}10\text{Na}_2\text{O}\text{-}2.5\text{Nd}_2\text{O}_3\text{-}(x)\text{NiO}$, $x = 0.5, 1.0, 1.5, 2.0, 2.5$ mol% have been achieved in the amorphous matrix by using melt quenching technique. TEM observation shows the nucleation of NiO NPs has non-spherical shape with average size around 4.9 nm. Compositional analysis (EDX) discovered the existence of Ni, O, Te, Na, Mg and Nd in the prepared samples. Differential thermal analysis showed that T_g at 338 °C, T_m in the range 530–540 °C, exothermic peak T_c at about 455 °C, glass stability (ΔS) and the Hruby (H_R) are $\Delta S > 100$ °C implies the glass system is regarded as stable and the value of H_R is 1.52. FTIR and Raman analysis have observed the involvement of all functional groups, and this study has confirmed that adding NiO content raises the quantity of non - bridging oxygen atoms. They revealed the presence of various groups such as bending vibrations of Te-O-Te, stretching vibration of TeO_4 and stretching NiO mode in a title of glass. The magnetic

Table 6

Magnetic parameters of glass system of $(72.5-x)\text{TeO}_2\text{-}15\text{MgO}\text{-}10\text{Na}_2\text{O}\text{-}2.5\text{Nd}_2\text{O}_3\text{-}(x)\text{NiO}$, where $0 \leq x \leq 2.5$ mol%.

Sample No.	$\text{Ms}(\text{emu/g})$	$\text{Mr} \times 10^{-3} (\text{emu/g})$	$\text{Hc}(\text{Oe})$	Mr/Ms
0.5NiO	0.023 ± 0.001	3.51 ± 0.176	610 ± 30.5	0.153 ± 0.008
1.0NiO	0.063 ± 0.003	6.47 ± 0.324	349 ± 17.45	0.103 ± 0.005
1.5NiO	0.079 ± 0.001	1.88 ± 0.094	336 ± 16.8	0.024 ± 0.001
2.0NiO	0.164 ± 0.008	2.49 ± 0.125	125 ± 6.25	0.015 ± 0.001
2.5NiO	0.084 ± 0.004	6.00 ± 0.300	139 ± 6.95	0.071 ± 0.004

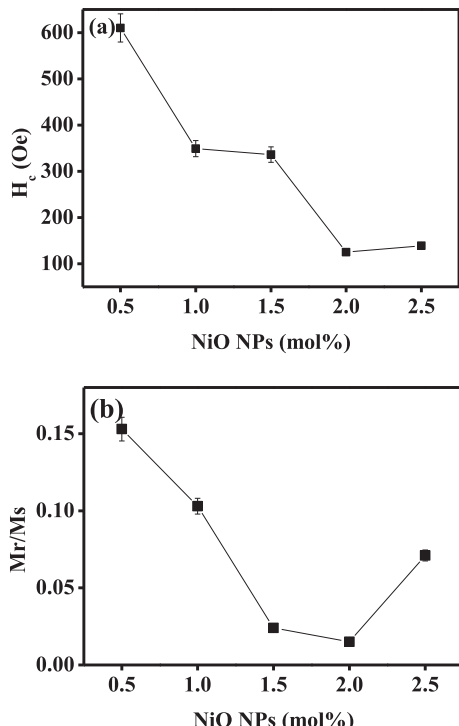


Fig. 8. (a) The variation of H_c as a function of NiO NPs concentration. (b) The variation of Mr/Ms . as a function of NiO NPs concentration.

measurements showed that the existence of NiO NPs in a glass specimen is paramagnetic behaviour at room temperature (25°C) and H_c values were observed to be decreased from 610 ± 30.5 to 139 ± 6.95 (Oe) and ratio of (Mr/Ms) from 0.153 ± 0.008 to 0.071 ± 0.004 with the increase NiO NPs concentration indicates that the materials are in multidomain magnetic grains composed in the glass structure.

Acknowledgements

The authors gratefully acknowledge the financial support from Universiti Teknologi Malaysia and Ministry of Higher Education, Malaysia through the Vot. 16H41, 05H45, 4F752 and 4L657.

Declaration of Competing Interests

The authors declare that they have no known competing financial interests or personal relationships that could have appeared to influence the work reported in this paper.

References

- [1] N.S. Hussain, G. Hungerford, R. El-Mallawany, M. Gomes, M. Lopes, N. Ali, J. Santos, S. Buddhudu, Absorption and emission analysis of RE^{3+} (Sm^{3+} and Dy^{3+}): lithium boro tellurite glasses, *J. Nanosci. Nanotechnol.* 9 (2009) 3672–3677.
- [2] R. El-Mallawany, A. Abd El-Moneim, Comparison between the elastic moduli of tellurite and phosphate glasses, *Phys. Status Solidi A* 166 (1998) 829–834.
- [3] R. El-Mallawany, Longitudinal elastic constants of tellurite glasses, *J. Appl. Phys.* 73 (1993) 4878–4880.
- [4] R. El-Mallawany, G. Saunders, Elastic behaviour under pressure of the binary tellurite glasses $\text{TeO}_2\text{-ZnCl}_2$ and $\text{TeO}_2\text{-WO}_3$, *J. Mater. Sci. Lett.* 6 (1987) 443–446.
- [5] R. El-Mallawany, Specific heat capacity of semiconducting glasses: binary vanadium tellurite, *Phys. Status Solidi A* 177 (2000) 439–444.
- [6] Y. Gandhi, N.K. Mohan, N. Veeraiah, Role of nickel ion coordination on spectroscopic and dielectric properties of $\text{ZnF}_2\text{-As}_2\text{O}_3\text{-TeO}_2\text{-NiO}$ glass system, *J. Non-Cryst. Solids* 357 (2011) 1193–1202.
- [7] A.A.A. Awshah, H.M. Kamari, C.K. Tim, N.M. Shah, S. Alazoumi, U.S. Aliyu, A. Azis, M. Noorazlan, Effect of neodymium nanoparticles on elastic properties of zinc-tellurite glass system, *Adv. Mater. Sci. Eng.* 2017 (2017) 1–7.
- [8] T. Xu, F. Chen, S. Dai, X. Shen, X. Wang, Q. Nie, C. Liu, K. Xu, J. Heo, Glass formation and third-order optical nonlinear properties within $\text{TeO}_2\text{-Bi}_2\text{O}_3\text{-BaO}$ pseudo-ternary system, *J. Non-Cryst. Solids* 357 (2011) 2219–2222.
- [9] D. He, S. Kang, L. Zhang, L. Chen, Y. Ding, Q. Yin, L. Hu, Research and development of new neodymium laser glasses, *High Power Laser Sci. and Eng.* vol. 5, (2017) 1–6.
- [10] P. Morkel, K. Jedrzejewski, E. Taylor, Q-switched neodymium-doped phosphate glass fiber lasers, *IEEE J. Quantum Electron.* 29 (1993) 2178–2188.
- [11] L. Bolundut, L. Pop, M. Bosca, N. Tothazan, G. Borodi, E. Culea, P. Pascauta, R. Stefan, Structural, spectroscopic and magnetic properties of Nd^{3+} doped lead tellurite glass ceramics containing silver, *J. Alloys Compd.* 692 (2017) 934–940.
- [12] R.S. Yadav, J. Havlicka, J. Masliko, L. Kalina, J. Wasserbauer, M. Hajdúchová, V. Enev, I. Kuřítká, Z. Kožáková, Impact of Nd^{3+} in CoFe_2O_4 spinel ferrite nanoparticles on cation distribution, structural and magnetic properties, *J. Magn. Magn. Mater.* 399 (2016) 109–117.
- [13] C. Yu, Z. Yang, J. Zhao, J. Zhu, A. Huang, J. Qiu, Z. Song, D. Zhou, Luminescence enhancement and white light generation of Eu^{3+} and Dy^{3+} single-doped and co-doped tellurite glasses by Ag nanoparticles based on Ag⁺-Na⁺ ion-exchange, *J. Alloys Compd.* 748 (2018) 717–729.
- [14] K. Karthik, S. Dhanuskodi, C. Gobinath, S. Prabukumar, S. Sivaramakrishnan, Nanostructured CdO-NiO composite for multifunctional applications, *J. Phys. Chem. Solids* 112 (2018) 106–118.
- [15] Y. Mahaleh, S. Sadirnezhad, D. Hosseini, NiO nanoparticles synthesis by chemical precipitation and effect of applied surfactant on distribution of particle size, *J. Nanomater.* 2008 (2008) 78.
- [16] G. Vijayaprasath, R. Murugan, S. Palanisamy, N. Prabhu, T. Mahalingam, Y. Hayakawa, G. Ravi, Role of nickel doping on structural, optical, magnetic properties and antibacterial activity of ZnO nanoparticles, *Mater. Res. Bull.* 76 (2016) 48–61.
- [17] M. Ghosh, K. Biswas, A. Sundaresan, C. Rao, MnO and NiO nanoparticles: synthesis and magnetic properties, *J. Mater. Chem.* 16 (2006) 106–111.
- [18] J. Richardson, D. Yiagas, B. Turk, K. Forster, M. Twigg, Origin of superparamagnetism in nickel oxide, *J. Appl. Phys.* 70 (1991) 6977–6982.
- [19] N. Mironova-Ulmane, A. Kuzmin, I. Steins, J. Grabis, I. Sildos, M. Pärs, Raman scattering in nanosized nickel oxide NiO, *J. Phys. Conf. Ser.* 93 (2007) 012039.
- [20] N. Dharmaraj, P. Prabu, S. Nagarajan, C. Kim, J. Park, H. Kim, Synthesis of nickel oxide nanoparticles using nickel acetate and poly (vinyl acetate) precursor, *Mater. Sci. Eng. B* 128 (2006) 111–114.
- [21] L. Barrientos, S. Rodriguez-Llamazares, J. Merchaní, P. Jara, N. Yutronic, V. Lavayen, Unveiling the structure of Ni/Ni oxide nanoparticles system, *J. Chil. Chem. Soc.* 54 (2009) 391–393.
- [22] S. Tiwari, K. Rajeev, Magnetic properties of NiO nanoparticles, *Thin Solid Films* 505 (2006) 113–117.
- [23] T. Ahmad, K.V. Ramanujachary, S.E. Lofland, A.K. Ganguli, Magnetic and electrochemical properties of nickel oxide nanoparticles obtained by the reverse-micellar route, *Solid State Sci.* 8 (2006) 425–430.
- [24] S.Z. Khan, Y. Yuan, A. Abdolvand, M. Schmidt, P. Crouse, L. Li, Z. Liu, M. Sharp, K. Watkins, Generation and characterization of NiO nanoparticles by continuous wave fiber laser ablation in liquid, *J. Nanopart. Res.* 11 (2009) 1421–1427.
- [25] M.R. Sahar, N.A. Mat Jan, Physical properties and band gap modification of neodymium doped tellurite glass embedded with NiO nanoparticles, *J. of Solid State Sci. and Technol.* 17 (2016) 1–7.
- [26] S. Elazoumi, H. Sidek, Y. Rammah, R. El-Mallawany, M. Halimah, K. Matori, M. Zaid, Effect of PbO on optical properties of tellurite glass, *Results in phys.* 8 (2018) 16–25.
- [27] M. Azlan, M. Halimah, Y. Azlina, S. Umar, R. El-Mallawany, G. Najmi, Linear and non-linear optical efficiency of novel neodymium nanoparticles doped tellurite glass for advanced laser glass, *EDUCATUM J. of Sci., Math. and Technol. (EJSMT).* 5 (2018) 47–66.
- [28] J.A. Creighton, D.G. Eadon, Ultraviolet-visible absorption spectra of the colloidal metallic elements, *J. Chem. Soc. Faraday Trans.* 87 (1991) 3881–3891.
- [29] T. Isobe, S.Y. Park, R.A. Weeks, R.A. Zuhri, The optical and magnetic properties of Ni

- + – implanted silica, *J. Non-Cryst. Solids* 189 (1995) 173–180.
- [30] G. Carja, A. Nakajima, C. Dranca, K. Okada, Nanoparticles of nickel oxide: growth and organization on zinc-substituted anionic clay matrix by one-pot route at room temperature, *J. Nanopart. Res.* 12 (2010) 3049–3056.
- [31] A.A. El-Moneim, DTA and IR absorption spectra of vanadium tellurite glasses, *Mater. Chem. Phys.* 73 (2002) 318–322.
- [32] S.X. Shen, A. Jha, Raman spectroscopic and DTA studies of TeO₂-ZnO-Na₂O tellurite glasses, *Adv. Mater. Res.* 39 (2008) 159–164.
- [33] W. Jordan, A. Jha, A review of the role of DSC analysis in the design of fluorozirconate glasses for fibre optic applications, *J. Therm. Anal.* 42 (1994) 759–770.
- [34] R. El-Mallawany, I.A. Ahmed, Thermal properties of multicomponent tellurite glass, *J. Mater. Sci.* 43 (2008) 5131–5138.
- [35] E. Culea, S. Rada, M. Rada, P. Pascuta, V. Maties, Structural and electronic properties of tellurite glasses, *J. Matter Sci.* 44 (2009) 3235–3240.
- [36] D. Varshney, S. Dwivedi, Synthesis, structural, Raman spectroscopic and paramagnetic properties of Sn doped NiO nanoparticles, *Superlattice. Microst.* 86 (2015) 430–437.
- [37] D. Srivastava, V. Pol, O. Palchik, L. Zhang, J. Yu, A. Gedanken, Preparation of stable porous nickel and cobalt oxides using simple inorganic precursor, instead of alkoxides, by a sonochemical technique, *Ultrason. Sonochem.* 12 (2005) 205–212.
- [38] S. Rada, M. Culea, E. Culea, Structure of TeO₂-B₂O₃ glasses inferred from infrared spectroscopy and DFT calculations, *J. Non-Cryst. Solids* 354 (2008) 5491–5495.
- [39] Y.B. Saddeek, E.R. Shaaban, K.A. Aly, I.M. Sayed, Characterization of some lead vanadate glasses, *J. Alloys Compd.* 478 (2009) 447–452.
- [40] J. Sabadel, P. Armand, D. Cachau-Herreillat, P. Baldeck, O. Doclot, A. Ibanez, E. Philippot, Structural and nonlinear optical characterizations of tellurium oxide-based glasses: TeO₂-BaO-TiO₂, *J. Solid State Chem.* 132 (1997) 411–419.
- [41] H. Fares, I. Jlassi, H. Elhouichet, M. Férid, Investigations of thermal, structural and optical properties of tellurite glass with WO₃ adding, *J. Non-Cryst. Solids* 396 (2014) 1–7.
- [42] A. Kaur, A. Khanna, M. González-Barriuso, F. González, B. Chen, Short-range structure and thermal properties of alumino-tellurite glasses, *J. Non-Cryst. Solids* 470 (2017) 14–18.
- [43] A. Jha, S. Shen, M. Naftaly, Structural origin of spectral broadening of 1.5-μm emission in Er³⁺-doped tellurite glasses, *Phys. Rev. B* 62 (2000) 6215.
- [44] A. Dehelean, S. Rada, A. Popa, R. Suciu, E. Culea, Raman, photoluminescence and EPR spectroscopic characterization of europium (III) oxide-lead dioxide-tellurite glassy network, *J. Lumin.* 177 (2016) 65–70.
- [45] V. Kamalaker, G. Upender, C. Ramesh, V. Chandra Mouli, Raman spectroscopy, thermal and optical properties of TeO₂-ZnO-Nb₂O₅-Nd₂O₃ glasses, *Spectrochim. Acta A Mol. Biomol. Spectrosc.* 89 (2012) 149–154.
- [46] S.A.M. Azmi, M. Sahar, S. Ghoshal, R. Arifin, Modification of structural and physical properties of samarium doped zinc phosphate glasses due to the inclusion of nickel oxide nanoparticles, *J. Non-Cryst. Solids* 411 (2015) 53–58.
- [47] G.U. Swapna, V. Sreenivasulu, M. Prasad, Spectroscopic and optical properties of the VO₂⁺ ion doped TeO₂-TiO₂-ZnO-Nb₂O₅ glass system, *J. Korean Phys. Soc.* 68 (2016) 998–1007.
- [48] M.R. Sahar, N.A. Mat Jan, Influence of NiO nanoparticles on magnetic properties of neodymium doped tellurite glasses, *Solid State Phenom.* 268 (2017) 102–105.
- [49] S.A.M. Azmi, M. Sahar, Optical response and magnetic characteristic of samarium doped zinc phosphate glasses containing nickel nanoparticles, *J. Magn. Magn. Mater.* 393 (2015) 341–346.
- [50] M. Naseri, A. Dehzangi, H.M. Kamari, A. See, M. Abedi, R. Salasi, A.N. Goli-Kand, P. Dianat, F. Larki, A. Abedini, Structure and physical properties of NiO/Co₃O₄ nanoparticles, *Metals.* 6 (2016) 181.
- [51] W. Widanarto, M. Sahar, S. Ghoshal, R. Arifin, M. Rohani, M. Effendi, Thermal, structural and magnetic properties of zinc-tellurite glasses containing natural ferrite oxide, *Mater. Lett.* 108 (2013) 289–292.
- [52] P. Anigrahawati, M. Sahar, S. Ghoshal, Influence of Fe₃O₄ nanoparticles on structural, optical and magnetic properties of erbium doped zinc phosphate glass, *Mater. Chem. Phys.* 155 (2015) 155–161.
- [53] S.E. Shirasath, B. Toksha, K. Jadhav, Structural and magnetic properties of In³⁺ substituted NiFe₂O₄, *Mater. Chem. Phys.* 117 (2009) 163–168.
- [54] J. Coey, Rare Earth Permanent Magnetism, vol. 1, John Wiley and Sons, 1996, p. 220.
- [55] L. Zhang, Y. Zhang, Fabrication and magnetic properties of Fe₃O₄ nanowire arrays in different diameters, *J. Magn. Magn. Mater.* 321 (2009) L15–L20.
- [56] R. Bhowmik, V. Vasanthi, A. Poddar, Alloying of Fe₃O₄ and Co₃O₄ to develop Co_{3x}Fe_{3(1-x)}O₄ ferrite with high magnetic squareness, tunable ferromagnetic parameters, and exchange bias, *J. Alloys Compd.* 578 (2013) 585–594.
- [57] K. Praveena, K. Sadhana, H.S. Virk, Structural and magnetic properties of Mn-Zn ferrites synthesized by microwave-hydrothermal process, *Solid State Phenom.* 232 (2015) 45.